

Water-Soluble J-Type Rosette Nanotubes with Giant Molar Ellipticity

Gabor Borzsonyi,^{†,‡} Rachel L. Beingessner,[†] Takeshi Yamazaki,[†] Jae-Young Cho,[†]
Andrew J. Myles,[†] Marek Malac,^{†,§} Ray Egerton,^{†,§} Masahiro Kawasaki,[⊥] Kazuo Ishizuka,[#]
Andriy Kovalenko,^{†,||} and Hicham Fenniri^{*,†,||}

National Institute for Nanotechnology, Departments of Chemistry, Physics, and Mechanical Engineering, University of Alberta, 11421 Saskatchewan Drive, Edmonton, Alberta, T6G 2M9, Canada., JEOL USA, Inc., 11 Dearborn Road, Peabody, Massachusetts 01960, and HREM Research, 14-48 Matsukazedai, Higashimastuyama, 355-0055, Japan

Received June 9, 2010; E-mail: hicham.fenniri@ualberta.ca

Abstract: A new self-assembling *tricyclic* module ($\times K1$) featuring the Watson–Crick H-bonding arrays of guanine and cytosine fused to an internal pyridine ring was synthesized. When dissolved in water at room temperature, this module rapidly self-assembles into hexameric rosettes, which then stack to form J-type rosette nanotubes (RNTs) with increased inner/outer diameters and the largest molar ellipticity ever reported ($4 \times 10^6 \text{ deg} \cdot \text{M}^{-1} \cdot \text{m}^{-1}$). Using a combination of imaging and spectroscopic techniques we established the structure of $\times K1$ -RNT and have shown that the extended π system of the self-assembling module resulted in a new family of J-type RNTs with enhanced inter-modular electronic communication.

Since their discovery in 1936 by Scheibe¹ and Jelley,² J-aggregates³ have seen a broad range of applications because they display coherent, cooperative phenomena such as superradiance and giant oscillator strength as a result of the long-range delocalization of their electronic excitation.^{3a,4} J-aggregates have for example been used as organic photoconductors,⁵ optical switches,⁶ NLO devices,⁷ critically coupled resonators,⁸ LEDs,⁹ sensitizers,¹⁰ photovoltaics,¹¹ nanowires,¹² and sensors.¹³

J-aggregates are usually dye crystallites in which the transition dipoles of the constituent molecules strongly couple to form a collective narrow line width optical transition possessing oscillator strength derived from the aggregated monomers.¹⁴ In this report we use self-assembly and self-organization strategies¹⁵ to build water-soluble J-type nanotubular architecture with unprecedented control over dimensions, supramolecular organization, and physical properties relative to earlier reports on J-aggregates. This approach offers opportunities for further tunability of electronic properties through subtle changes in the core structure and functionalization of the self-assembling molecular modules.

The G \wedge C motif¹⁶ is a self-complementary hybrid molecule of the DNA bases guanine and cytosine. This motif and its derivatives¹⁷ (**2**, Figure 1) were studied extensively in water and organic solvents and were shown to undergo hierarchical self-assembly into hexameric rosettes which further organize into a linear stack called a rosette nanotube (RNT).^{16c,18} Here we present a water-soluble *tricyclic* variant **1**, termed $\times K1$. This molecule features the same H-bonding arrays, but separated by an internally fused pyridine ring. Building upon the design criteria formulated and successfully

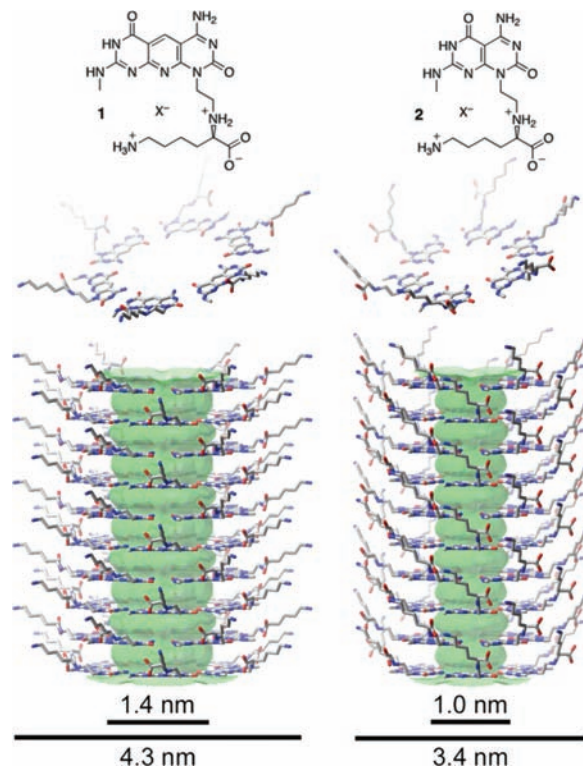


Figure 1. $\times K1$ (**1**) and $K1$ (**2**) modules, corresponding hexameric rosettes (middle), and RNTs (lower) ($X = \text{CF}_3\text{CO}_2^-$).

established in the case of its bicyclic congener, $\times K1$ was specifically designed to (a) self-assemble in water to form RNTs with increased inner/outer diameters relative to $K1$ (**2**) and (b) engender an extended π system that would enhance electronic transport along the RNT's main axis.

Following is the synthesis, self-assembly, and characterization of $\times K1$ using circular dichroism (CD), UV–vis and fluorescence spectroscopy, scanning electron microscopy (SEM), transmission electron microscopy (TEM), tapping mode atomic force microscopy (TM-AFM), energy filtering TEM (EFTEM), off-axis electron holography (EH), and quantitative phase technology (QPt). We also report remarkable optical properties suggesting enhanced electronic communication for this new class of RNTs.

The synthesis of $\times K1$ (Scheme 1) began by transforming commercially available barbituric acid in three steps to bicycle **3**. Three consecutive regioselective $\text{S}_{\text{N}}\text{Ar}$ reactions at positions 4, 2, and 7 with benzyl alcohol, methylamine, and allylamine, respectively, provided the functionalized compound **6**. However, for the third $\text{S}_{\text{N}}\text{Ar}$ reaction to proceed, it was necessary to electronically

[†] National Institute for Nanotechnology, University of Alberta.

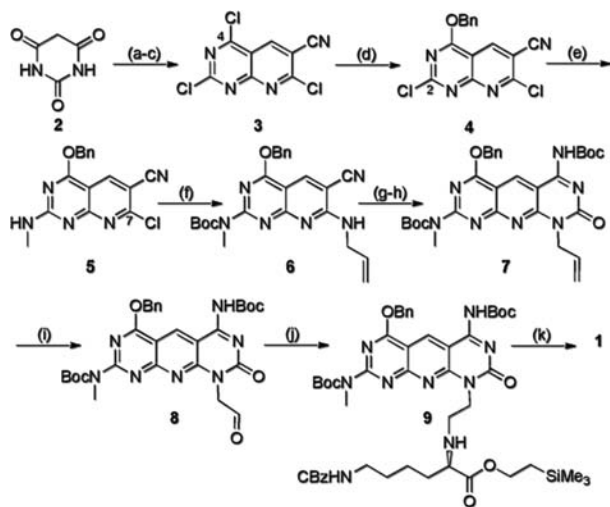
[‡] Department of Chemistry, University of Alberta.

[§] Department of Physics, University of Alberta.

[⊥] Department of Mechanical Engineering, University of Alberta.

[⊥] JEOL USA, Inc.

[#] HREM Research.

Scheme 1. Synthesis of $\times K1^a$ 

^a (a) POCl_3 , DMF, reflux, 15 h, 90%; (b) malonitrile, β -alanine, CH_3CN , 30 h, 50%; (c) 180°C , 48 h, 75%; (d) BnOH , Et_3N , CH_2Cl_2 , -40°C , 2 h, 70%; (e) CH_3NH_2 (2 M in THF), DIPEA, CH_2Cl_2 , 0°C , 2 h, 60%; (f) Boc_2O , DIPEA, DMAP, THF, rt (room temperature), 12 h then allylamine, DIPEA, CH_2Cl_2 , rt, 2 h, 50%; (g) Cl_3CONCO , CH_2Cl_2 , rt, 5 h then 7 N NH_3 in MeOH, rt, 12 h, 74%; (h) Boc_2O , DIPEA, DMAP, THF, rt, 12 h, 96%; (i) OsO_4 in *t*-BuOH, 50% NMO in H_2O , THF, rt, 6 h, then NaIO_4 in H_2O , rt, 48 h, 85%; (j) Protected L-Lysine, DIPEA, 1,2-DCE, rt, 10 min, then $\text{Na}(\text{OAc})_3\text{BH}$, rt, 48 h, 82%; (k) 94/6 (v/v) TFA/thioanisole, rt, 96 h, 87%.

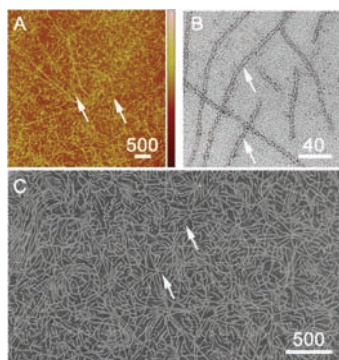


Figure 2. Imaging of $\times K1$ RNTs (0.1 mg/mL in water) by (A) TM-AFM (5 μm scan, height scale = 0–10 nm), (B) TEM, and (C) SEM. White arrows point to individual RNTs; scale bars in nm.

deactivate the ring by protecting the methylamine in compound **5** with an electron-withdrawing group. Ring closure of **6** using trichlorocarbonyl isocyanate/ NH_3 , followed by protection of the amine, generated tricycle **7**. Oxidative cleavage of alkene **7** and

subsequent reductive amination of aldehyde **8** with protected L-lysine provided compound **9**. Finally, deprotection of **9** with TFA/thioanisole furnished the target $\times K1$ motif (**1**) as a TFA salt.

Characterization of $\times K1$ by SEM revealed that this tricyclic compound rapidly self-assembles into RNTs when dissolved in water ($\text{pH}_{\text{final}} = 2.8$) (Figure 2C) at room temperature. This is an advantage over the bicyclic $G\wedge C$ base **2** which requires heat to drive the entropically driven self-assembly process as a result of its reduced hydrophobic character.^{18b} TM-AFM (Figure 2A) and TEM (Figure 2B) of uranyl acetate-stained samples established the RNTs' outer diameter of 4.2 ± 0.2 and 4.4 ± 0.2 nm, respectively, in excellent agreement with the theoretical value 4.3 nm. These measurements were further verified using three direct TEM imaging methods (without staining agent), from which the diameter of a single RNT was measured to be 4.5 ± 1 nm (EFTEM), 4.4 ± 0.75 nm (EH), and 4.9 ± 0.8 nm (QPt).¹⁹ In contrast with EFTEM, EH and QPt use elastic scattering of the fast electrons in TEM instead of the inelastically scattered electrons to obtain quantitative measurements. Based on these results, the inner and outer diameters of $\times K1$ -RNTs relative to $K1$ -RNTs increased by 0.4 and 0.9 nm, respectively.

CD and UV-vis spectroscopic techniques were used to monitor the self-assembly process in solution. The CD spectra of $\times K1$ (2.1×10^{-5} M) feature two couplets centered at 257 and 380 nm with positive maxima at 264 and 388 nm (Figures 3B). The CD signal intensity increased *ca.* 40 \times over 7 days reaching a giant molar ellipticity, with an unprecedented value of $4 \times 10^6 \text{ deg}\cdot\text{M}^{-1}\cdot\text{m}^{-1}$ for a chiral helical stack.²⁰ Briefly heating a dilute solution of $\times K1$ (1.9×10^{-5} M) to 100°C (10 s) or acidification with TFA (0.1% v/v) leads to the complete disappearance of the CD profile, thus suggesting that the induced CD is the result of the supramolecular chirality of the RNTs. In agreement with these studies, variable temperature CD (VT-CD) established the reversibility of the CD profile.¹⁹ The intensity of the CD couplet is proportional to the fourth power of the dipole strength and the relative orientation of the chromophores and is inversely proportional to the square of the interchromophoric distance.²¹ Since the latter is probably the same for RNTs assembled from $K1$ and $\times K1$, the very large molar ellipticity recorded is therefore an indication of the much larger transition dipole strength and an optimal relative orientation of the corresponding dipole moments.

UV-vis, CD, and fluorescence spectroscopy unveiled the remarkable optical properties of the RNTs assembled from $\times K1$ ($\times K1$ -RNT). First, the UV-vis spectra of $K1$ versus $\times K1$ show a significant shift of all the maxima toward the red in the latter case. $K1$ showed maxima at 236 and 285 nm, whereas $\times K1$ showed maxima at 246 and 363 nm in addition to a unique, sharp, and lower energy band at 388 nm (Figure 3A). This band is unique to

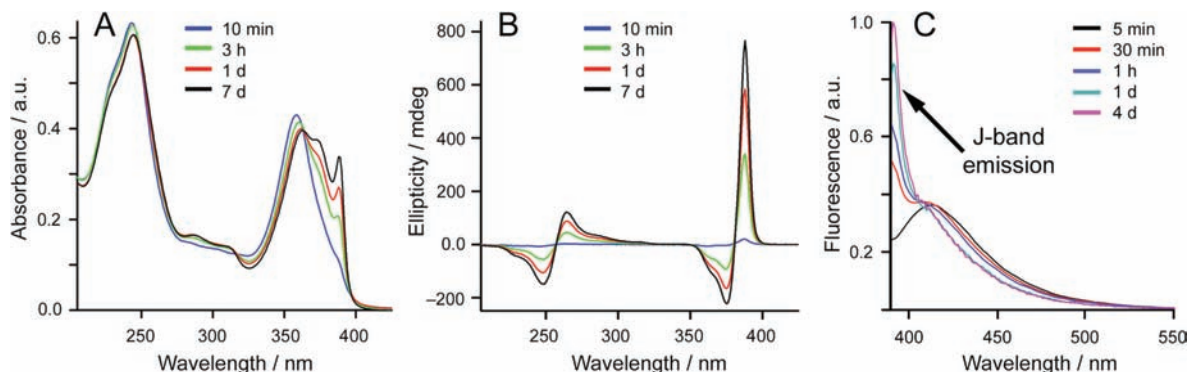


Figure 3. (A) UV-vis, (B) circular dichroism, and (C) fluorescence ($\lambda_{\text{exc}} = 388$ nm) spectra of $\times K1$ -RNTs (*ca.* 2×10^{-5} M in water).

×K1-RNT as it has never been observed for bicyclic GAC derivatives such as K1^{16c,18} or nonassembled ×K1. Because this band is narrow and red-shifted and grew over time and because it decreased with increasing temperature (Figures S3, S4), dilution (Figures S5, S6),¹⁹ or titration with TFA (data not shown), we propose that ×K1 modules assumed a J-type arrangement^{1–3} within the RNTs.

Second, the growth of the J-band is associated with the growth of a couplet centered on the same λ_{max} (388 nm) (Figures 3B, S2). Variable temperature UV–vis and CD showed that this couplet is associated with the supramolecular organization of ×K1-RNT, as it disappears with heating and grows upon cooling (Figure S4).

Third, a subtle hypochromic effect (*ca.* 8%) was observed over 7 days (Figure 3A) whereas a pronounced hyperchromic effect (up to *ca.* 50%) was recorded upon thermally induced disassembly (Figure S5).¹⁹ While this result suggests that RNT formation has already substantially progressed prior to the initial measurements (*i.e.*, within minutes), the UV–vis and CD profiles, notably the appearance and growth of the red-shifted band along with the CD couplet, suggest that the formation of J-type RNTs proceeds in at least two stages: the first step (within minutes) leading to rapid formation of RNTs and the second (within days) during which ×K1 modules adopt a particularly favorable supramolecular arrangement for exciton coupling within the RNT construct. We refer to these states as conformational states I and II (CS-I, CS-II). As evidenced by time-dependent SEM,¹⁹ the shape, dimension, and hierarchy/aggregation states of ×K1-RNTs were the same in CS-I and CS-II. However, the transition from CS-I to CS-II clearly has a dramatic effect on the relative orientation of the transition dipoles of the self-assembling modules and their exciton delocalization.³

To further establish the J-type nature of ×K1-RNTs, steady-state fluorescence spectroscopy was carried out. Three excitation wavelengths were used to observe the changes in emission upon transition from CS-I to CS-II, namely the λ_{max} of CS-I (356 nm), the isosbestic point (369 nm), and the λ_{max} of the J-band (388 nm) for CS-II. The time-dependent emission spectra resulting from excitation at 356 and 369 nm showed a decrease in fluorescence intensity and a change in band shape due to the growth of the narrow J-band fluorescence peak at 393 nm (Figures S7, S8). Excitation of the J-band at 388 nm minimizes the absorption of CS-I and shows growth of the J-band fluorescence emission at 393 nm (Figure 3C). The absorption and emission spectra are nearly mirror image and the Stokes shift for the J-band is only 5 nm, consistent with the formation of J-type aggregates.²² In addition, the emission of CS-II (relative to CS-I) is more intense possibly as a result of an increased quantum yield of the J-aggregate.

As is the case for J-type aggregates, the remarkably strong CD couplet observed for ×K1 coincides with the newly formed red-shifted J-band and is likely due to coupling of stronger electric dipole transitions between adjacent molecules in the RNTs.²¹ This may stem from the higher polarizability, larger π electron system, and supramolecular arrangement of the dipole moments of ×K1 relative to its parent module **2**, whose effect is 3-fold: (a) it increases the hydrophobic/amphiphilic character of ×K1, which results in stronger assemblies in water and polar solvents; (b) it promotes stronger and larger π – π interactions, which are favorable to establishing optimal interchromophoric distances and geometries for exciton coupling; and (c) it increases electronic delocalization.

In summary, here we describe the design, synthesis, and characterization of a new class of water-soluble RNTs from a *tricyclic* self-assembling module (×K1). UV–vis and CD experiments revealed interesting optical properties. In particular, the formation of highly ordered J-type RNTs suggests long-range intermodular electronic communication relative to the parent RNTs (derived from **2**). Detailed photophysical studies to determine the size of the coherent domain of the J-aggregates within the ×K1-RNTs are underway. Our results suggest also that by further extending the ring system of the GAC motif, we should be able to realize an electronically conducting RNT with tremendous practical and fundamental potential.^{4–13}

Acknowledgment. We thank NSERC, NRC, and the University of Alberta for supporting this program.

Supporting Information Available: Synthetic procedures for ×K1; UV–vis, CD and fluorescence studies; SEM, TEM, AFM, EH, QP and EFTEM procedures and studies; and computational methods. This material is available free of charge via the Internet at <http://pubs.acs.org>.

References

- (1) Scheibe, G. *Angew. Chem.* **1936**, *49*, 563.
- (2) Jelley, E. E. *Nature* **1936**, *138*, 1009.
- (3) (a) Möbius, D. *Adv. Mater.* **1995**, *7*, 437. (b) Kuhn, H.; Kuhn, C. In *J-Aggregates*; Kobayashi, T., Ed.; World Scientific: Singapore, 1996; Chapter 1. (c) Mishra, A.; Behera, R. K.; Behera, P. K.; Mishra, B. K.; Behera, G. B. *Chem. Rev.* **2000**, *100*, 1973.
- (4) Kobayashi, T., Ed. *J-Aggregates*; World Scientific: Singapore, 1996.
- (5) (a) Lin, H.; Camacho, R.; Tian, Y.; Kaiser, T. E.; Würthner, F.; Scheblykin, I. G. *Nano Lett.* **2010**, *10*, 620. (b) Jin, W.; Yamamoto, Y.; Fukushima, T.; Ishii, N.; Kim, J.; Kato, K.; Takata, M.; Aida, T. *J. Am. Chem. Soc.* **2008**, *130*, 9434. (c) Law, K. -Y. *Chem. Rev.* **1993**, *93*, 449. (d) Eisele, D. M.; Knoester, J.; Kirstein, S.; Rabe, J. P.; Vanden Bout, D. A. *Nat. Nano.* **2009**, *4*, 658. (e) Borsenberger, P. M.; Chowdry, A.; Hoesterey, D. C.; Mey, W. *J. Appl. Phys.* **1978**, *44*, 5555.
- (6) (a) Zheng, J.; Qiao, W.; Wan, X.; Gao, J. P.; Wang, Z. Y. *Chem. Mater.* **2008**, *20*, 6163. (b) Sasaki, F.; Kobayashi, S. *Appl. Phys. Lett.* **1993**, *63*, 2887. (c) Tian, M.; Tatsuura, S.; Furuki, M.; Sato, Y.; Iwasa, I.; Pu, L. S. *J. Am. Chem. Soc.* **2003**, *125*, 348. (d) Adhikari, R. M.; Shah, B. K.; Palayangoda, S. S.; Neckers, D. C. *Langmuir* **2009**, *25*, 2402.
- (7) (a) Wang, Y. *Chem. Phys. Lett.* **1986**, *126*, 209. (b) Wang, Y. *J. Opt. Soc. Am. B* **1991**, *8*, 981. (c) Kobayashi, S. *Mol. Cryst. Liq. Cryst.* **1992**, *217*, 77.
- (8) Tischler, J. R.; Bradley, M. S.; Bulovic, V. *Opt. Lett.* **2006**, *31*, 2045.
- (9) (a) Tischler, J. R.; Bradley, M. S.; Zhang, Q.; Atay, T.; Nurmikko, A.; Bulovic, V. *Org. Electron.* **2007**, *8*, 94. (b) Walker, B. J.; Nair, G. P.; Marshall, L. F.; Bulovic, V.; Bawendi, M. G. *J. Am. Chem. Soc.* **2009**, *131*, 9624.
- (10) James, T. H., Ed. *The Theory of the Photographic Process*; Macmillan: New York, 1977.
- (11) (a) Sayama, K.; Tsukagoshi, S.; Mori, T.; Hara, K.; Ohga, Y.; Shinpou, A.; Abe, Y.; Suga, S.; Arakawa, H. *Sol. Energy Mater. Sol. Cells* **2003**, *80*, 47. (b) Kawasaki, M.; Aoyama, S. *Chem. Commun.* **2004**, 988. (c) Tameev, A. R.; Vannikov, A. V.; Schoo, H. F. M. *Thin Solid Films* **2004**, *451/452*, 109. (d) Meng, F.; Chen, K.; Tian, H.; Zuppiroli, L.; Nuesch, F. *Appl. Phys. Lett.* **2003**, *82*, 3788. (e) Steiger, R.; Pugin, R.; Heier, J. *Colloids Surf., B* **2009**, *74*, 484. (f) Zhang, Q.; Atay, T.; Tischler, J. R.; Bradley, M. S.; Bulovic, V.; Nurmikko, A. V. *Nat. Nano.* **2007**, *2*, 555. (g) Wang, X.-F.; Kitao, O.; Zhou, H.; Tamiaki, H.; Sasaki, S. *J. Phys. Chem. C* **2009**, *113*, 7954. (h) Spitzer, M. T.; Parkinson, B. A. *Acc. Chem. Res.* **2009**, *42*, 2017.
- (12) Lagoudakis, P. G.; de Souza, M. M.; Schindler, F.; Lupton, J. M.; Feldmann, J. *Phys. Rev. Lett.* **2004**, *93*, 257401–1.
- (13) Whitten, D. G.; Achyuthan, K. E.; Lopez, G. P.; Kim, O.-K. *Pure Appl. Chem.* **2006**, *78*, 2313.
- (14) Vanburgel, M.; Wiersma, D. A.; Duppen, K. *J. Chem. Phys.* **1995**, *102*, 20.
- (15) (a) Lehn, J.-M. *Science* **2002**, *295*, 2400. (b) Whitesides, G. M.; Simanek, E. E.; Mathias, J. P.; Seto, C. T.; Chin, D. N.; Mammen, M.; Gordon, D. M. *Acc. Chem. Res.* **1995**, *28*, 37. (c) Cornelissen, J. J. L. M.; Rowan, A. E.; Nolte, R. J. M.; Sommerdijk, N. A. J. M. *Chem. Rev.* **2001**, *101*, 4039. (d) Lawrence, D. S.; Jiang, T.; Levett, M. *Chem. Rev.* **1995**, *95*, 2229. (e) Prins, L. J.; Reinhoudt, D. N.; Timmerman, P. *Angew. Chem., Int. Ed.* **2001**, *40*, 2382. (f) Shimizu, T.; Masuda, M.; Minamikawa, H. *Chem. Rev.* **2005**, *105*, 1401.
- (16) (a) Marsh, A.; Silvestri, M.; Lehn, J.-M. *Chem. Commun.* **1996**, 1527. (b) Mascal, M.; Hext, N. M.; Warmuth, R.; Moore, M. H.; Turkenburg, J. P. *Angew. Chem., Int. Ed. Engl.* **1996**, *35*, 2204. (c) Fenniri, H.; Mathivanan, P.; Vidale, K. L.; Sherman, D. M.; Hallenga, K.; Wood, K. V.; Stowell, J. G. *J. Am. Chem. Soc.* **2001**, *123*, 3854.
- (17) (a) Beingessner, R.; Deng, B.-L.; Fanwick, P. E.; Fenniri, H. *J. Org. Chem.* **2008**, *73*, 931. (b) Tikhomirov, G.; Oderinde, M.; Makeiff, D.; Mansouri,

- A.; Weibing, L.; Heitzler, F. R.; Kwok, D. Y.; Fenniri, H. *J. Org. Chem.* **2008**, *73*, 4248.
- (18) (a) Fenniri, H.; Deng, B.-L.; Ribbe, A. E. *J. Am. Chem. Soc.* **2002**, *124*, 11064. (b) Fenniri, H.; Deng, B.-L.; Ribbe, A. E.; Hallenga, K.; Jacob, J.; Thiagarajan, P. *Proc. Natl. Acad. Sci. U.S.A.* **2002**, *99*, 6487. (c) Moralez, J. G.; Racz, J.; Yamazaki, T.; Motkuri, R. K.; Kovalenko, A.; Fenniri, H. *J. Am. Chem. Soc.* **2005**, *127*, 8307. (d) Johnson, R. S.; Yamazaki, T.; Kovalenko, A.; Fenniri, H. *J. Am. Chem. Soc.* **2007**, *129*, 5735. (e) Moralez, J. G.; Racz, J.; Fenniri, H. *J. Am. Chem. Soc.* **2004**, *126*, 16298. (f) Yamazaki, T.; Fenniri, H.; Kovalenko, A. *ChemPhysChem* **2010**, *11*, 361.
- (19) See Supporting Information.
- (20) (a) Kim, O.-K.; Je, J.; Jernigan, G.; Buckley, L.; Whitten, D. *J. Am. Chem. Soc.* **2006**, *128*, 510. (b) Nuckolls, C.; Katz, T. J.; Castellanos, L. *J. Am. Chem. Soc.* **1996**, *118*, 3767. (c) von Berlepsch, H.; Kirstein, S.; Böttcher, C. *J. Phys. Chem. B* **2003**, *107*, 9646.
- (21) Berova, N.; Di Bari, L.; Pescitelli, G. *Chem. Soc. Rev.* **2007**, *36*, 914.
- (22) Chan, J. M. W.; Tischler, J. R.; Kooi, S. E.; Bulovic, V.; Swager, T. M. *J. Am. Chem. Soc.* **2009**, *131*, 5659.

JA105028W